SIMULATION OF LONGITUDINAL PHASE SPACE IN THE SLC*

Karl L. F. Bane
Stanford Linear Accelerator Center, Stanford University, Stanford, CA 94309 USA

INTRODUCTION

Upon leaving the damping ring, the SLC beam passes through the Ring-to-Linac transfer line (RTL), the linac, and the arcs on its way to the collision point. In an earlier paper [1] calculations of the longitudinal distributions of the lengthened damping ring beam were presented, calculations that agreed remarkably well with measurements. In this paper we propagate the damping ring distributions through the rest of the machine. Among the effects that are included in the calculations are the curvature of the compressor rf and the limited energy aperture in the RTL, the wakefields in the linac, and the momentum compaction in the arcs. More details can be found in Ref. 2.

THE RTL

Bunch Compression

In a bunch compressor the beam first enters an rf section on the zero crossing of the rf wave (with particles in front gaining energy, those in back losing energy) and secondly traverses a dispersive beam line. The net result is a shorter beam with a larger energy spread. Note that bunch compression in the SLC is discussed in Refs. 3-5.

Let us describe bunch compression by a transformation of the initial beam coordinates (z,δ) to the final coordinates (u,v). Here as elsewhere in this paper a more negative value of position is more toward the front of the bunch; in addition, energy coordinates are given in units of relative energy deviation from the mean. Let us assume the beam position $z=0$ enters the compressor on the zero crossing of the rf wave. For the moment let us, in addition, assume the compressor rf wave is linear. Then bunch compression is described by

$$v = -az + \delta \quad \text{and} \quad u = z + bv = \alpha z + b\delta \quad , \qquad (1)$$

with $\alpha = 1-ab$. The compressor rf strength factor a is given by $a = eV_c k_{rf}/E_0$, with V_c the peak amplitude of the compressor rf wave, k_{rf} the rf wave number, and E_0 the average beam energy, and b the momentum compaction.

The bunch distribution function $f(z,\delta)$ transforms to the new distribution function $g(u,v)$ as

$$f(z,\delta)\,dz\,d\delta = g(u,v)\,du\,dv = f(z,\delta)J(z,\delta;u,v)\,du\,dv \qquad (2)$$

with J the Jacobian for the transformation. Our transformation is area preserving and $J(z,\delta;u,v)=1$. Therefore,

$$g(u,v) = f(z,\delta) = f(u-bv, au+\alpha v) \quad . \qquad (3)$$

The final position and energy distributions are

$$\lambda_u(u) = \int g(u,v)\,dv \quad \text{and} \quad \lambda_v(v) = \int g(u,v)\,du \quad . \qquad (4)$$

We assume that the initial (*i.e.* damping ring) distribution function is separable as $f(z,\delta) = \lambda_z(z)\lambda_\delta(\delta)$, with λ_z and λ_δ representing respectively the initial position and energy distributions. Therefore the final distribution function is given by

$$g(u,v) = \lambda_z(u-bv)\lambda_\delta(au+\alpha v) \quad . \qquad (5)$$

Several familiar properties of bunch compression can be derived by substituting Eq. (5) into Eq. (4). We see that at full compression, when $\alpha = 0$, $\lambda_u = a\lambda_\delta(au)$. If, in addition the beam energy spread is greatly increased in the process of compression (as is normal), then $\lambda_v = b\lambda_x(-bv)$. When $\alpha \neq 0$ and assuming that both λ_δ and λ_z are gaussian, with the respective lengths σ_δ and σ_z, we see that the final position and energy distributions are also gaussian with lengths [4]

$$\sigma_u = \sqrt{\alpha^2\sigma_z^2 + b^2\sigma_\delta^2} \quad \text{and} \quad \sigma_v = \sqrt{a^2\sigma_z^2 + \sigma_\delta^2} \quad . \qquad (6)$$

We are mostly interested in the compressor behavior near full compression, i.e. where $\alpha\sigma_z \lesssim b\sigma_\delta$.

The damping ring bunch length increases with current; at higher currents the full length of the bunch approaches half the wavelength of the compressor rf. We will include the effects of the curvature of the compressor rf by replacing az in the transformation equations Eq. (1) by $(eV_c/E_0)\sin k_{rf}z$. Then

$$g(u,v) = \lambda_z(u-bv)\,\lambda_\delta(v + [eV_c/E_0]\sin k_{rf}[u-bv]) \quad . \qquad (7)$$

Simulation Results

We begin our simulations with the damping ring distributions, λ_z and λ_δ. To obtain the bunch shape λ_z a modified version of potential well theory is used [1]. Since the damping ring impedance is inductive the bunch lengthens with current. As for the energy distribution λ_δ, it is taken to be gaussian. Below the threshold current for instability N_{th} the energy spread is taken to be constant, above threshold it varies as $N^{1/3}$. For a complete description of the damping ring calculations see Ref.1. Nominally the ring operates at a voltage $V_{ring} = 1$ MV, and in our calculations we will limit ourselves to this voltage. The nominal (low current) bunch length is 4.42 mm, the nominal energy spread is 0.07%. We will take $N_{th} = 1.9\times10^{10}$. To obtain the final distributions we substitute the ring distributions into Eq. (7), then into Eqs. (4) and then integrate numerically. The energy aperture limits of the RTL (at least on the North side) are $\pm2.25\%$ [6]; we therefore set the limits of integration over dv to these values. Note that for the RTL $b = 0.603$ m, $E_0 = 1.15$ GeV, and $k_{rf} = 60$ m^{-1}.

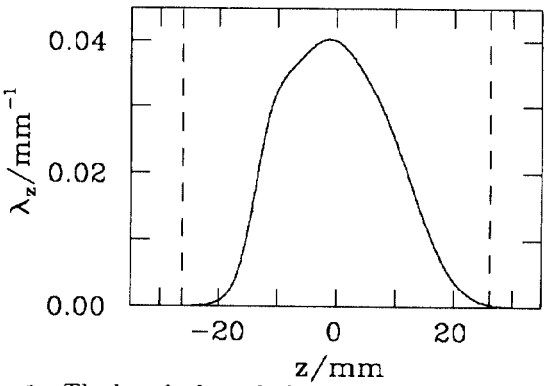

Figure 1. The bunch shape before compression, when $N = 5\times10^{10}$ and $V_{ring} = 1$ MV.

As an example, consider a beam with $N = 5\times10^{10}$. The initial (*i.e.* damping ring) energy distribution is gaussian with a spread $\sigma_\delta = 0.1\%$. The initial position distribution, with the beam centered on the zero crossing of the compressor rf, is shown in Fig. 1. The dashes locate the nearest extrema of the rf wave. The rms bunch length $z_{rms} = 8.7$ mm and the full-width(-at-half-maximum) $\Delta z_{FW} = 25.3$ mm. These values are respectively twice and 2.5 times the nominal values. Far from the beam core the tails of the distribution become gaussian. These tails, however, are centered on the nominal synchronous point in the ring, which is 4.2 mm to the right of beam center.

If we set $V_c = 30$ MV we obtain the results shown in Fig. 2. Fig. 2c shows contours of phase space; the dashed curve gives the ridge line of the distribution. The dotted lines mark the limits of the $\pm2.25\%$ energy aperture; 4% of the beam lies outside these limits, and is lost. Fig. 2a shows the final energy distribution. This curve is similar to, though more rectangular

* Work supported by Department of Energy contract DE-AC03-76SF00515.

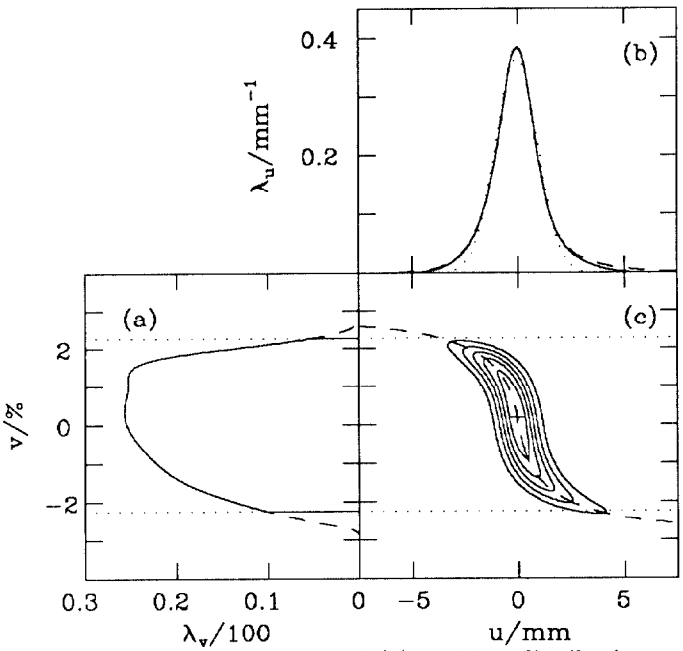

Figure 2. (a) The energy and (b) position distributions, and (c) contours of phase space, after bunch compression. For this example $N = 5 \times 10^{10}$, and $V_c = 30$ MV.

than, the mirror image of the initial bunch shape (see Fig.1). The distribution essentially fills the energy aperture. Its rms width $v_{rms} = 1.17\%$, its full-width $\Delta v_{FW} = 4.04\%$. In contrast, for a low current beam, the spectral shape is almost gaussian with $v_{rms} = 0.7\%$ [see Eq. (6)], and therefore $\Delta v_{FW} = 1.65\%$.

Fig. 2b displays the final bunch shape. As expected the shape is similar to that of the initial energy distribution, *i.e.* similar to a gaussian. The dotted curve gives a gaussian fit to the bunch shape, with an rms length of $\sigma_{ug} = 1.0$ mm. The dashed curve shows the position distribution when there is no limitation in the energy aperture. In Fig. 3 we plot again the same three curves of Fig. 2b, but this time showing in more detail the tails. In the bunch distribution (the solid curve) we see notches in both tails, a result of the energy collimation. The asymmetry in the distribution reflects the asymmetry of the tails of the initial distribution λ_z. The distribution when the energy aperture limitation is removed (the dashed curve) has tails that vary roughly as $e^{-c_1 u}$, with c_1 a constant, rather than as a gaussian (the dots), due to the rf curvature.

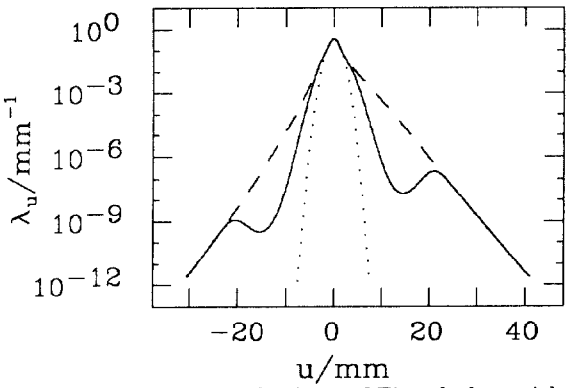

Figure 3. The bunch distributions of Fig. 2b, but with the axes expanded to show the behavior in the tails.

We have repeated the calculations for various currents and compressor settings. The length of the gaussian fit to the resulting bunch shapes σ_{ug} is plotted as function of V_c and as function of N in Fig. 4. The voltage that gives the minimum bunch length increases from 33 MV to 34 MV as we increase the current from 0 to 6×10^{10}. In contrast the linear rf approximation has its minimum at 32 MV. The dotted curve in Fig. 4a gives the low current, linear rf result. Finally, recall that under the linear rf approximation and with $\alpha = 0$ the final bunch length is given by the initial energy spread, $\sigma_u = b\sigma_\delta$. The dotted curve in Fig. 4b shows this approximation.

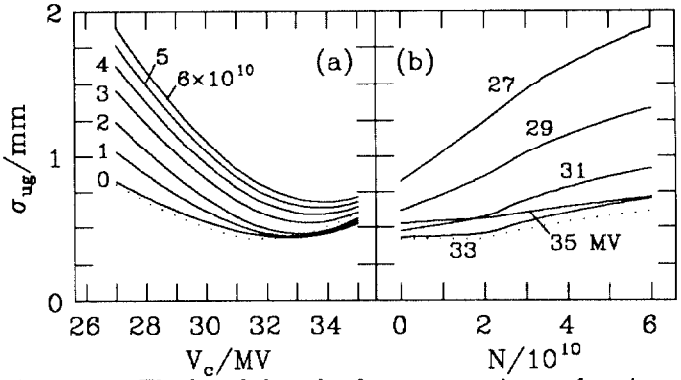

Figure 4. The bunch length after compression as function of (a) V_c and (b) N. The parameter σ_{ug} is the rms of the gaussian fit to the position distribution λ_u.

THE LINAC

The shape of the beam spectrum at the end of the SLC linac has been studied by many authors (*e.g.* Refs. 7-10). For a detailed description of the spectral properties of the bunch at the end of the linac as function of current, bunch length, and rf phase see Ref. 10.

The transformation to the final linac position and energy coordinates (u', v') is described by

$$u' = u \quad \text{and} \quad v' = \frac{E_0}{E_f} v + \bar{v}(u) \quad , \tag{8}$$

with E_f the final average energy. Normally the function

$$\bar{v}(u) = \frac{1}{E_f} \left[E_0 + E_a \cos(k_{rf} u + \phi) + e V_{ind}(u) \right] - 1 \quad , \tag{9}$$

with E_a the total peak rf energy gain, ϕ the beam phase with respect to the rf crest, and V_{ind} the induced voltage in the linac, gives essentially all the longitudinally correlated energy variation. The final position and energy distributions are

$$\lambda_{u'} = \lambda_u \text{ and } \lambda_{v'} = \frac{E_f}{E_0} \int \lambda_u(u') \, \lambda_v \left(\frac{E_f}{E_0} [v' - \bar{v}(u')] \right) du' \, . \tag{10}$$

Note that parentheses in the above equation surround the argument of a function.

If E_f/E_0 is large then the function λ_v in the integral of Eq. (10) is much more sharply peaked as function of u' than is λ_u. We can, therefore, approximate

$$\lambda_{v'} = \sum_w \lambda_u(w) / \left| \frac{d\bar{v}}{dw}(w) \right| \quad \text{with} \quad w = \bar{v}^{-1}(v') \quad . \tag{11}$$

The sum in this equation indicates that if the inverse function $\bar{v}^{-1}$ is multivalued at v' then all contributions must be summed. According to Eq. (11) wherever $d\bar{v}/du' = 0$ the energy distribution has an infinitely high spike. In reality, however, the distribution must be everywhere finite, and the minimum width of any spike is given by the width of the uncorrelated component of the energy variation.

Consider again the case $N = 5 \times 10^{10}$ and $V_c = 30$ MV. The total length of accelerating structure (needed for finding V_{ind}) is 2744 m. The acceleration gradient is chosen to give $E_f = 47$ GeV. The induced voltage, found by convolving the bunch shape with the wakefield for the SLAC structure [11], is given in Fig. 5. Then, since λ_u and λ_v are known from our earlier calculation, we obtain the final energy spectrum by performing the integration of Eq. (10).

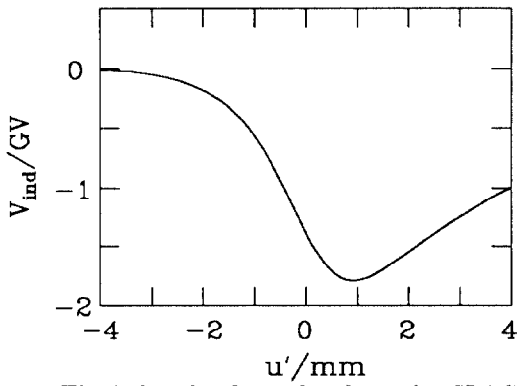

Figure 5. The induced voltage for the entire SLAC linac, when $N = 5 \times 10^{10}$ and $V_c = 30$ MV.

Fig. 6 displays the final spectrum when the beam is positioned at 5° and at 10° in front of the rf crest. The dashed curves, with their scales on the right, give $\bar{v}(u')$. At the top of the crest, the spectrum has two, widely-separated spikes. As the beam is moved forward the core of the spectrum narrows, and tails begin to grow. At its narrowest the spectrum full-width is $\Delta v'_{FW} = 0.06\%$. To optimize the luminosity we roughly want to maximize the number of particles within an energy window of $\pm 0.5\%$. (See Ref. 10 for more details.) For our examples 44% and 87% of the original beam are within this window; we find that $-10°$ is near the optimal phase.

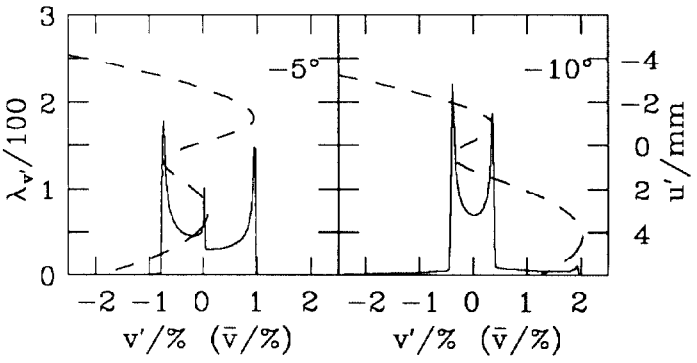

Figure 6. The bunch spectrum at the end of the linac $\lambda_{v'}$ for two values of rf phase. $N = 5 \times 10^{10}$ and $V_c = 30$ MV.

THE ARCS

Since the SLC arcs have non-zero momentum compaction the bunch shape will change in the arcs. Note that bunch compression in the arcs is discussed in Ref. 12. The transformation of a point at the end of the linac (u', v') to its position at the end of the arcs (u'', v'') is

$$u'' = u' + b_{arc} v' \quad \text{and} \quad v'' = v' \quad , \tag{12}$$

with b_{arc} the arc compaction factor. The final distributions

$$\lambda_{u''} = \int \lambda_{u'}(u'' - b_{arc} v'') \lambda_{v'}(v'')\, dv'' \text{ and } \lambda_{v''} = \lambda_{v'} \ . \tag{13}$$

If E_f/E_0 is large then we can approximate

$$\lambda_{u''} = \sum_s \lambda_u(s) / |\frac{dh}{ds}(s)| \quad \text{with} \quad s = h^{-1}(u'') \quad , \tag{14}$$

and $h(u) = u + b_{arc}\bar{v}(u)$. The bunch shape will have a spike wherever the denominator in Eq. (14) is zero. Again the spikes must be finite, with the minimum width of any spike given by b_{arc} times the width of the uncorrelated component of energy variation. Note also that wherever the slope of $\bar{v}(u)$ is negative the bunch will compress, wherever it is positive the bunch will expand. In our case the beam core will tend to compress and the tails expand. Note that if $\bar{v}(u) = c_1 u$, with c_1 a constant, then the final distribution is given by the initial distribution, but with its width scaled by the factor $(1 + b_{arc} c_1)$.

We numerically solve Eq. (13) to obtain the bunch shape after the arcs. The compaction parameter b_{arc} is 0.145 m. Synchrotron radiation in the arcs will smear the final bunch shape by an rms of 0.08 mm; we include this effect by convolving the bunch shape with a gaussian of this length. (Note the final spectrum is also smeared, by 0.08%.) At the top of the crest, the bunch distribution has two spikes that narrow as the beam is moved forward. Without synchrotron radiation the narrowest full-width would be 0.09 mm, with synchrotron radiation it is limited to 0.21 mm. For the same examples of Fig. 6 we show the final bunch shape in Fig. 7. The dashed curves give the final energy/position correlation, $\bar{v}(u'') \equiv \bar{v}(u'' - b_{arc} v')$. For our two examples the full-widths of the bunch shape $\Delta u''_{FW}$ are 0.92 mm and 0.23 mm; the fraction of beam in the core $n_{u''c}$ is 75% and 50%.

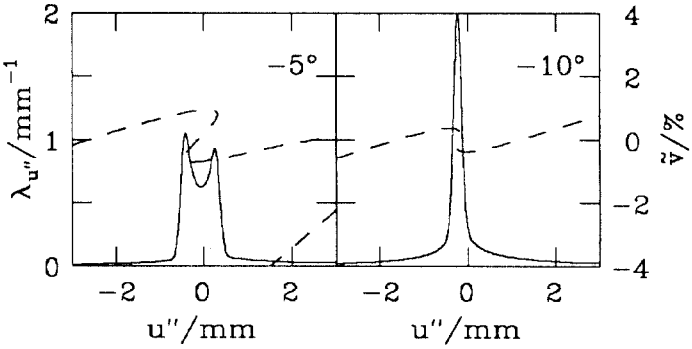

Figure 7. The bunch shape at the end of the arcs $\lambda_{u''}$ for two values of rf phase. $N = 5 \times 10^{10}$ and $V_c = 30$ MV.

Table 1 displays results for other currents, when $V_c = 30$ MV, for phases that yield near optimal luminosity. Included are the linac bunch length σ_{ug} and rf phase ϕ; the full-width and core population of the beam spectrum at the end of the linac, $\Delta v'_{FW}$ and $n_{v'c}$, and of the bunch shape at the end of the arcs, $\Delta u''_{FW}$ and $n_{u''c}$. We see that, in all these cases, the final bunch length $\Delta u''_{FW}$ is near the minimum possible value.

Table 1. Results for different currents. $V_c = 30$ MV.

N (10^{10})	σ_{ug} (mm)	$-\phi$ (deg)	$\Delta v'_{FW}$ (%)	$n_{v'c}$	$\Delta u''_{FW}$ (mm)	$n_{u''c}$
2	0.70	7	0.50	0.90	0.25	0.65
3	0.85	8	0.65	0.85	0.25	0.55
4	0.95	9	0.75	0.85	0.25	0.55
5	1.05	10	0.80	0.80	0.25	0.50

ACKNOWLEDGMENTS

The author thanks M. Ross, J. Seeman, W. Spence, R. Warnock, and members of the SLC Linac Group for having contributed to his understanding of this subject.

REFERENCES

[1] K. Bane and R. Ruth, Proc. of the 1989 IEEE Particle Acc. Conf., Chicago, 1989, p. 789.
[2] K. Bane, SLAC-AP-80 (1990).
[3] T. Fieguth, SLAC-CN-79 (1981).
[4] H. Wiedemann, SLAC-CN-117, (1981).
[5] The SLC Design Handbook p. 6-33 (1984).
[6] SLC Linac Log Book, Dec. 1987.
[7] R. Stiening, SLAC-CN-110 (1981).
[8] The SLC Design Handbook p. 2-21 (1984).
[9] J. Seeman and J. Sheppard, SLAC-PUB-3944 (1988).
[10] K. Bane, SLAC-AP-76 (1989).
[11] K. Bane and P.B. Wilson, Proc. of the 11th Int. Conf. on High-Energy Acc., CERN (1980), p. 592.
[12] A.W. Chao and Y. Kamiya, SLAC-CN-218 (1983).